Hindawi
Advances in Civil Engineering
Volume 2019, Article ID 7676801, 15 pages
https://doi.org/10.1155/2019/7676801

Research Article

Study on Multiparameter Precursory Information Identification of the Fracture of Yellow Sandstone

Xiao Fukun, Wang Houran, and Liu Gang

Heilongjiang Ground Pressure and Gas Control in Deep Mining Key Lab, Heilongjiang University of Science and Technology, Haerbin 150022, China

Correspondence should be addressed to Liu Gang; 814449714@qq.com

Received 30 August 2018; Revised 1 December 2018; Accepted 10 December 2018; Published 17 January 2019

Guest Editor: Guo-Zhong Hu

In order to explore the disaster caused by uncontrollable instability of coal and rock mass, a multiparameter fusion system is constructed to predict and predict disasters more accurately by identifying the mechanical and acoustic precursors of coal and rock fracture. In order to explore the precursor information of yellow sandstone rupture, the damage evolution process of yellow sandstone is analyzed from the four aspects of rock mechanics, acoustic emission time domain, frequency domain, and characteristic parameters, and the body strain, dissipated energy and acoustic emission counting, acoustic emission energy, average frequency, peak frequency, *b* value, and entropy value precursor information identification points are obtained, and 8 parameters are analyzed by time series fusion. The specific conclusions are as follows: body strain in the violent stage of damage evolution, the slope is zero, the zero end point is the precursor information identification point, the dissipative energy curve overall shows the "s" type, the early growth rate is faster—the medium-term stability—the later period is slowed down, and the upper slope boundary point of the "s" type curve is used as the precursor information identification point. In the violent stage of damage evolution, the layered features of the acoustic emission count are obvious, the specific gravity shift is more obvious, and the high count appears as the precursor information identification point; the acoustic emission energy accumulates the high-energy signal and is accompanied by the steady and rapid growth of energy as the precursor information identification point. The effects of shearing main cracks, shear microcracks, tensile cracks, and composite cracks on the acoustic emission count and energy in the damage evolution process are analyzed. The increase of medium- and high-frequency signals and the reduction of high-frequency signals predict the rupture. The average frequency signal change law is continuous high frequency-blank-continuous high frequency, with the blank period end point as the damage precursor identification point; the *b* value damage evolution stage shows a continuously steady increase to a rapid increase, with the continuous stable growth starting point as the crack identification point. In the process of damage evolution, the sample entropy presents an orderly, chaotic, disordered, and orderly process. The end of chaos and the beginning of disorder are used as the prejudging demarcation points. Based on the time sequence, an eight-parameter comprehensive early warning system is constructed. The indicators are classified into five levels for early warning in the stage of severe damage evolution. The identification of multiparameter precursory information of yellow sandstone provides a new research idea and analysis angle and method for the failure of other coal and rock masses.

1. Introduction

With the development of underground engineering construction in China, there are more and more rock mechanics problems encountered. The focuses of attention are the stability and evaluation method of rock mass. The underground space is mixed with too many unknown conditions. It is difficult to accurately answer whether the rock is stable by theoretical analysis. Therefore, the characteristics of the process from stability to instability should be studied by monitoring methods, and the characteristic information of the prerupture period should be proposed to evaluate the stability of the rock mass. If there is a tendency to instability, we will take timely measures to ensure safety. Acoustic emission can accurately capture the elastic wave released by the crack development of coal and rock and can accurately evaluate the "healthy state" of rock mass. The acoustic emission waveform carried information about crack

development, and by its time domain and frequency domain analysis, we can grasp the stress state of the rock mass. When the rock mass is about to break, the crack development is disorderly, and the acoustic emission signal presents complexity and nonlinearity. The scholars propose the complexity of different time series based on the sample entropy. The entropy research is widely used in medical health assessment and mechanical fault diagnosis. There are few applications for rock mass fracture prediction. Based on the abnormal commonality, the sample entropy is introduced to study the precursor characteristics of rock mass instability failure. In the process of rock damage evolution, different stages show different characteristics. We should reasonably capture the characteristics of different stages and fuse features under the time order, in order to construct a complete early warning system.

In the process of instability analysis of coal rock based on acoustic emission, time domain analysis, frequency domain analysis, and characteristic parameter analysis are often used. The information that can be characterized and feed back by each method is different, and it has guiding significance for the prediction of instability failure. The time domain analysis mainly studies the variation of the parameters of acoustic emission waveform with loading time and stress growth and predicts the rupture by the abnormal changes (increasing, decreasing, and calming) in the early stage of the catastrophe. Scholars often use acoustic emission, counting, energy, energy rate, event, amplitude, duration, and average frequency to analyze it. Frequency domain analysis is mainly to study the dynamic characteristics and steady-state error of the acoustic emission waveform, and the peak frequency, average frequency, and main frequency change in the spectrum predict the instability; the characteristic parameters are the acoustic emission parameters mainly extracted by the mathematical theory and calculation method, the fractal dimension, b value, clustering, neural network which are more common. Through the prepeak variation of the characteristic parameters, we can study the early warning law.

In terms of time domain analysis of acoustic emission, Cao et al. [1] conducted uniaxial compression granite acoustic emission experiments and obtained the characteristics of acoustic emission energy and counting in the early stage of rupture. Yao et al. [2] conducted acoustic emission monitoring experiments on granite, marble, coal, and siltstone, and evaluated the instability of rock by energy contribution rate and event rate. Xu [3] has analyzed the number of acoustic emission ringing in the early stage of rupture of granulites, granites, and limestone. Shen [4] has carried out a uniaxial experiment on dry and water-containing coal samples and obtained the variation law of acoustic emission energy and counting of coal sample damage. Liu et al. [5, 6] carried out research on the acoustic emission law of combined coal rock rupture and the quantitative evaluation of granite damage.

In acoustic emission frequency domain analysis, Xu [3] analyzed the change law of EMD energy entropy of acoustic emission in the prophase of rupture of granulite, granite, and limestone. Zhang et al. [7–9] the application of high frequency and low frequency, the most sensitive frequency rate and the coefficient of variation of frequency and energy, frequency and frequency analysis of granite precursory information, and dry and saturated coal gangue rupture variation process of frequency. Zeng et al. [10] studied the correlation dimension and main frequency of AE amplitude in the early stage of gritstone rupture. Liu et al. [11] carried out the horizontal unloading test of the granite circular tunnel model and obtained the variation law of the frequency band during the process of rock damage evolution and rupture. Cong et al. [12] analyzed the acoustic emission count and fractal characteristics of marble under different stress paths. Zhang [13] studied the impact rate, duration, energy, amplitude, average frequency, RA value, and dominant frequency of acoustic emission in the early stage of rock failure. Ji et al. [14] studied the variation of peak frequency, high-frequency and low-frequency count and energy during granite fracture. Yang et al. [15] study on the red sandstone under the condition of unloading confining pressure strength, deformation, and fracture behavior of red sandstone failure process of acoustic emission spatial evolution.

The following are some of the studies conducted for acoustic emission characteristic parameter analysis. Xu [3] analyzed the variation of acoustic emission ringing count, peak frequency, and EMD energy entropy in the early stage of granulite, granite, and limestone rupture. Zhang [13] Study on the early failure of rock acoustic emission RA value. Zhang et al. [16, 17] proposed time density by signal clustering analysis, optimized the signal source by neural network, and measured the risk of rockburst with time density and applied the highest frequency, lowest frequency, sensitive frequency, and frequency coefficient of variation, and the energy, main frequency, and main frequency amplitude and b value are used to analyze the precursor information of granite rupture; the main frequency and information entropy change law of dry and saturated coal gangue rupture process. Liu et al. [18] conducted acoustic emission tests on the unloading damage of coal samples under different initial confining pressures and obtained the timing of acoustic emission, spatial distribution, and amplitude variation. Wei et al. [19, 20] studied the variation of energy parameters, event parameters, b value, and entropy of biaxial loading of rock with pores. Yukai [21] studied on AE amplitude and ring of coal and rock failure. Zhao [22] studied acoustic emission b value during slip of prefabricated defective granite layered structure.

The following are some of the studies conducted for precursor evolution of rock mechanics: Lu [21] studied on the evolution law of AE energy of coal and rock instability and failure. Zhao et al. [22] studied the evolution of events during rock rupture. Liu et al. [11] carried out the horizontal unloading test of the granite circular tunnel model and obtained the variation law of the frequency band during the process of rock damage evolution and rupture. Hu et al. [24] studied by TBM in the process of excavation of tunnel surrounding rock acoustic emission characteristics, using acoustic emission parameters of surrounding rock damage law for evolution analysis. Xiao et al. [25–28] studied the energy conversion mechanism and acoustic characteristics

of coal and rock mass during loading. Lei [23] studied the evolution of events during the slip process of prefabricated defective granite layered structure. Yang [29] studied the mechanical properties and damage evolution of sandstone under cyclic loading and analyzed the tensile fracture and shear failure by CT technology. These research results have guiding significance for the analysis of rock failure and precursor damage, but nobody studies the rock instability precursors with the damage rupture, time domain, frequency domain, and characteristic parameters combined. The rock failure process will cause a variety of anomalies, and multiple analysis angles will help to dig deeper into the precursory information of the fracture.

The randomness of cracks is difficult to express and judge. The sample entropy is of great significance for the study of stochastic systems and random sequences. According to this, the paper refers to the method to predict the instability of characteristic parameters. As the crack penetrates, the rupture scale becomes larger and larger, and the b value is introduced according to the principle of seismology to analyze the precursor characteristics of rock failure. Through the statistical analysis of the scholars' research results, the acoustic emission count and energy analysis are used to analyze the evolution process of rock mass rupture in the time domain; the acoustic emission peak frequency and average frequency are extracted in the frequency domain to analyze the evolution process of rock mass rupture. Precursor information on rock damage evolution is obtained through deformation and energy. Based on this, a precursory information recognition system with four angles and eight parameters is constructed, and stability evaluation and early warning are carried out through parameter anomalies and timing.

2. Experimental Methods

2.1. Experimental Sample Preparation. In order to ensure the reference of the experimental results, the yellow sandstone is processed according to the method for determining the deformation parameters of coal and rock (GB/T 23561.8-2009), the standard size is $\varphi 50 \times 100$ mm, and the density of the block is determined by the wax sealing method to be 2.16 g/cm^3. The uniaxial compression deformation test measured the strength of 74.8 MPa, the elastic modulus was 12.8 GPa, and Poisson's ratio was 0.28. The internal structure was detected by industrial CT, and the yellow sandstone was homogeneous and compact. Using rock sample ultrasonic to test the test piece, the average value of P wave velocity is 3907 m/s, and the average value of S wave velocity is 2674 m/s, which can ensure the reliable exploration of the test pieces. The basic information of the rock sample is shown in Table 1. Since there are many rock samples, only the typical analysis is selected to give specific information. The fracture morphology of the triaxial experimental rock sample is shown in Figure 1. Due to space limitations, representative rock samples are selected for analysis. The basic information of the rock sample is shown in Table 1.

2.2. Experimental Equipment. The experiment uses the ROCK600-50 multifield coupling mechanics test system produced by TOP INDUSTRIE, France. The SH-II acoustic emission system is used to monitor the rock rupture process during the experiment. The composition and arrangement of the device are shown in Figure 2. In order to correct the rock breaking moment and information, the acoustic emission sensor 1 is arranged on the base of the press, and the whole process data of the loading and unloading is collected, and the acoustic emission sensor 2 is arranged on the side wall of the confining pressure chamber, because the signal is obviously attenuated in the hydraulic oil, only. An acoustic emission signal can be acquired when it is broken. The sensor is fixed in the corresponding position by a high-magnetic magnet. The Vaseline coupling sensor and the contact surface are used to ensure the time synchronization of the press and the acoustic emission. The clock calibration is performed before the experiment.

2.3. Experimental Plan. In the triaxial test process, the test piece is axially loaded by a servo pump, and after the deviatoric stress of 3 MPa is reached, the unloading is performed quickly to ensure that the axial indenter of the sample is in contact with the rock sample. The rock sample is loaded to a hydrostatic pressure of 5 MPa at a rate of 1 MPa/min. In order to ensure a stable transition of the rock sample system and to identify the acoustic emission effect, the hydrostatic pressure is maintained for a certain period of time, and then the deviatoric stress is increased at a rate of 1 MPa/min until the rock sample is destroyed. The acoustic emission is turned on during the deviatoric stress loading. In order to ensure the selection of the effective signal, the acoustic emission preamplifier is set to 40 dB, the indoor noise signal is less, the acoustic emission threshold is set to 35 dB, and the acoustic emission meter sampling frequency is set to 1 MHz. The sampling frequency is 1 MSPS, and the sampling length is 2K (1K = 1024). The acoustic emission sensor is Nano30 type with resonant high sensitivity, and the sensor operating frequency is 150~750 KHz. The experimental path is shown in Figure 3.

3. Extraction and Analysis of Precursor Information of Rock Fracture

There are obvious anomalies in the early stage of rock rupture, and the effects of analyzing the forecasts from different angles are inconsistent. The following is the extraction of precursor information from the perspective of rock sample mechanics, acoustic emission time domain, frequency domain, and characteristic parameters and gives the theory and basis and analyzes the precursor information to provide a theoretical basis for the early warning system construction.

3.1. Analysis of the Indicators of Deformation and Energy Angle Damage Precursors. Force is the direct cause of rock failure. Under the action of pressure, the deformation of rock sample is constantly changing, especially the plastic phase in

Table 1: Basic information of yellow sandstone.

Number	Diameter × height (mm)	Quality m (g)	Density (g/cm^3)	Confining pressure σ3 (MPa)	Elastic modulus (Pa)	Uniaxial compressive strength (MPa)	Poisson's ratio	S wave velocity (m/s)	P wave velocity (m/s)	Loading and unloading speed (MPa/min)
sz-17	50.30 × 100.10	434.7	2.13		12.7	74.5		2670	3895	
sz-18	50.02 × 100.02	436.2	2.19		12.9	75.1		2678	3927	
sz-20	50.19 × 101.61	436.4	2.12	5	12.6	74.2	0.28	2673	3908	1
sz-21	50.20 × 101.30	436.6	2.20		13	75.4		2675	3896	
sz-22	49.22 × 100.09	438.2	2.16		12.8	74.8		2674	3910	

Figure 1: Fracture photos of rock samples.

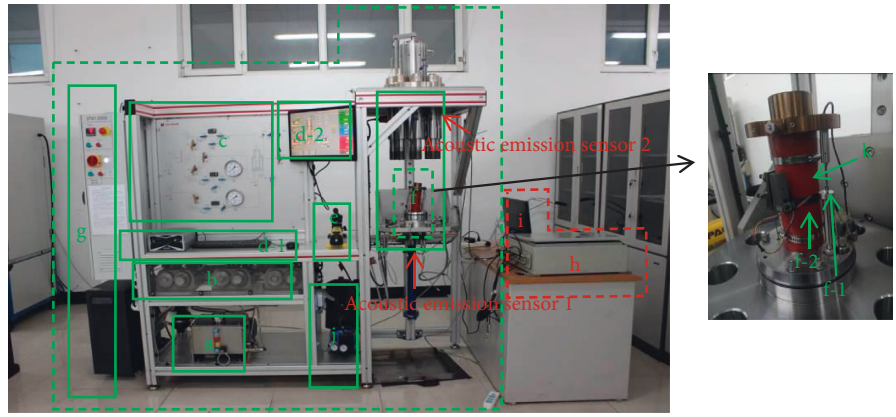

Figure 2: Synchronous unloading mechanical experiment device and acoustic acquisition device.

the early stage. At this time, the crack presents rapid initiation and local development. Grasping the deformation law at this stage has obvious warning function. Through the analysis of Figure 4, it is found that the axial strain and the radial strain have a synchronous plastic tendency, and the volumetric strain is in a constant state at a later stage, the prediction effect is later than the axial deformation and radial deformation, and the warning precursor information warning should be given in a small period of time before the rupture occurs. Therefore, it is too early to use the plastic starting point as a warning. It is of little significance. Take sample sz-20 as an example, the volumetric strain volume at constant time is 1085 s, the time of rock sample failure is 1186 s, and the precursor alert time is 138 s, total percentage 11.3% ahead of schedule and the plastic deformation time is 953 s and the advance warning is 233 s, advancing 19.6% of the total time. Through comparison, it is found that the starting point of plastic deformation is significantly earlier than the point of volume invariant of volume strain. The volumetric strain should be selected closer to the moment of failure, and the volumetric strain is a comprehensive feedback on axial deformation and radial deformation. The comprehensiveness of the deformation reaction is better. Accordingly, volumetric strain should be used in the selection of deformation precursor information.

The damage of rock damage is done under the action of stress and deformation. The press continuously supplies energy to the rock sample, and the rock sample continuously stores energy, and after the ultimate energy storage capacity is reached, the release of energy occurs. During the energy conversion process, part of energy is stored in the sample in the form of elastic energy, and part of it is consumed in the form of crack propagation. Figure 5 shows the energy conversion characteristics of the SZ-20 sample. By comparing the total energy accumulated before the peak and the energy released after the peak, it can be found that the

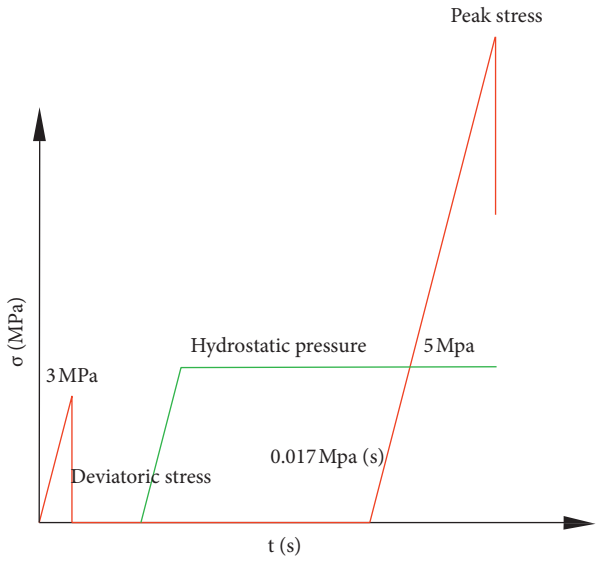

Figure 3: The experimental path.

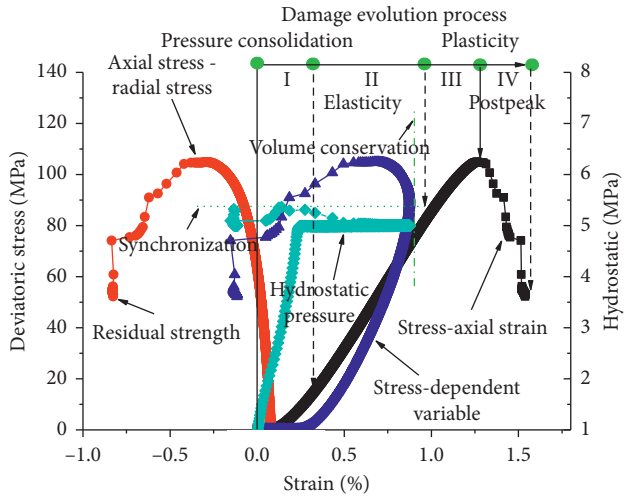

Figure 4: SZ-20 typical stress-strain damage evolution curve.

surplus energy appears and promotes the rock cracking process. The energy that can be discussed for the prepeak warning has total energy, elastic energy, and dissipated energy. Since the elastic energy presents a triangle, as the stress increases, the elastic energy increases continuously, it is difficult to grasp the change point, and it is not meaningful for extracting the precursor information. For the total energy accumulated before the peak, the warning effect cannot be judged by the intuitive angle. In the small image on the upper right corner of Figure 5, the abscissa is the strain, the ordinate is the total energy, and the stage auxiliary line is added. According to the green auxiliary line trend, the total energy in the middle and late period is nearly linear, and the precursor information is not significant enough, which brings difficulty to the warning, so the research on this parameter is abandoned. The energy dissipated by the crack energy itself is characterized by the expansion of the crack, and it can be clearly seen from the red region of Figure 5 that

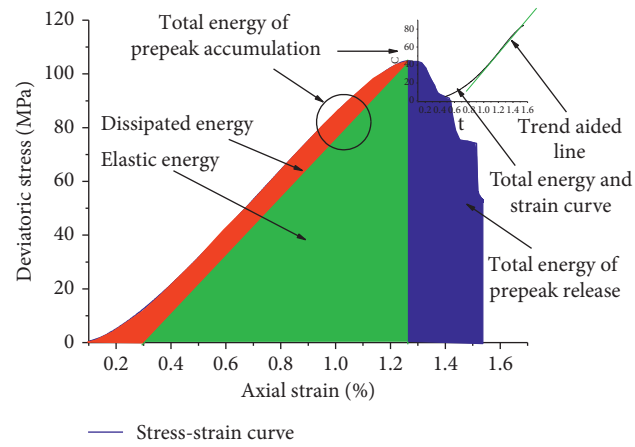

Figure 5: SZ-20 characteristics of energy conversion.

this part of the energy is constantly changing, especially in the later stage, which shows a significant narrowing trend. In summary, the dissipative energy is selected as the parameter of the energy angle precursor information identification.

3.2. Body Strain and Dissipative Energy Damage Precursor Research. Based on comprehensive considerations, body strain and dissipative energy were identified as objects for in-depth study. Figure 6 shows the curves of the strain-stress and damage evolution of five typical specimens with time. Observing the variation of the available strain curves is consistent. Both the early rise and the steady change of the body strain curve are derived from the initial hydrostatic pressure. Through the corresponding relationship between the pressure value and Figure 4, the damage evolution law of Figure 6 is calibrated. For the body strain, it is nearly linear in the local damage evolution stage (I and II); in the severe damage evolution stage (III), the body strain slope gradually decreases from a positive value to zero, and a negative value occurs after a certain period of time. The negative slope shows a certain acceleration growth trend until the rock sample is destroyed. How to find and determine the precursor information in the process of change has become the focus of the thesis. The analysis of the rock damage precursor must start from the third stage (the intense stage of damage evolution), and the process of the third stage is rock sample volume from reduction to constant to expansion. The purpose of the warning is to predict the disaster that will occur, and the early and late warnings cannot achieve the effect we want, so the volume reduction process is not considered. The volume expansion phase is short and rapid, and it is difficult to determine appropriate and reasonable warning points. In summary, the invariant end point of the volume should be defined as the precursor information identification point.

Taking the rock sample sz-18 as an example to illustrate the effect of body strain precursor recognition, the moment of rock sample failure is 1316 s, the corresponding pressure value is 113 MPa, the volume strain corresponding to the volume end point is 1.04%, the corresponding time is 1177 s, and the warning occurs 119 s ahead of the disaster for early

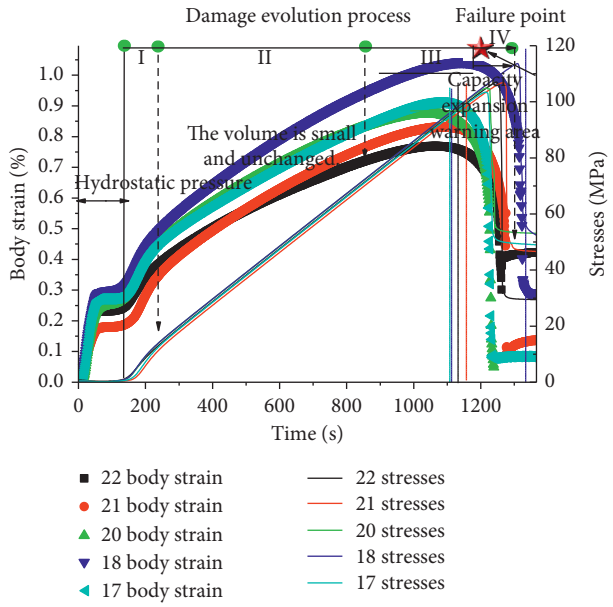

Figure 6: The relation curve of body strain stress and damage evolution process.

warning, and the relative loading to the damage process the warning time is 10.6%. The specific information is shown in Table 2, and the average value reached 11.4%.

The dissipative energy calculation takes the difference between the total energy and the elastic energy before the peak, and the two differential units are integrated to obtain the difference. Figure 7 shows the relationship between the sz-20 stress-strain curve and the evolution of the dissipative energy damage of the rock sample. The red region is the dissipative energy surrounded by the stress-strain curve. By adding a linear auxiliary line to the dissipative energy integral curve, the initial energy dissipation shows a gradual increase trend and reaches a certain position and then grows steadily. It appears in the first stage; after the dissipation energy reaches a certain value, the growth rate is steadily reduced, and the rupture moment reaches the extreme value. The dissipative energy curve generally exhibits the "s" type, and the growth rate in the early stage is fast-intermediately stable-later-slowing. The demarcation point of the slope of the "s"-shaped curve has a certain basis as the precursor information research area. Take the sz-20 curve as an example to illustrate the effect of dissipative energy precursor recognition. When the rock sample breaks down at 1223 s, the corresponding pressure value is 105 MPa, the energy consumed by the dissipative energy demarcation point is 8.79 KJ/m^3, the corresponding time is 1037 s, and the rupture occurs 186 s ahead of time for early warning. The warning time of relative loading to the damage process is 15.2%. Figure 8 shows the relationship between the dissipated energy and the strain. The variation of the dissipative energy curve has similarity. The magnitude of the dissipative energy release is proportional to the strain corresponding to the peak. Table 3 gives the prewarning warning information for dissipative energy, with an average of 7.8%.

3.3. Acoustic Emission Counting and Precursor Analysis of Energy Damage. Acoustic emission can effectively characterize the process, scale, and spatial location of crack propagation in coal and rock mass. A plurality of parameters is defined from different angles by receiving elastic waves of crack propagation. The basic principle is shown in Figure 9. The acoustic emission count is the number of oscillations after the waveform exceeds the threshold value. The energy is the area enclosed by the waveform envelope. Both can evaluate the scale of crack propagation, which has certain significance for the early warning of damage.

All characteristic parameters of acoustic emission are defined based on waveforms, and only the process of rock crack propagation is reflected from different angles. By comparing the acoustic emission parameters (absolute energy, energy, count, amplitude, effective voltage, average voltage, duration, and rise time) and reference data discovery, acoustic emission count and energy are the most sensitive indicators for rock damage. Figures 10 and 11 show the variation of acoustic emission count and energy during the loading process of samples 22 and 21. In the initial stage of damage evolution, the acoustic emission count is less than 200, the acoustic emission energy is low, and two concentrated jumps occur. In the middle stage of damage evolution, several high-energy signals appeared in a certain interval, and the sound emission count of sample 22 showed an increasing trend. The sound emission count of sample 21 showed a decreasing trend, and the proportion of high-counting signal gradually increased. The less the damage occurs, the layered features of the acoustic emission count become more and more obvious, and the specific gravity shift is more obvious, especially between 1000 and 2000. Therefore, at this stage, the interval is divided by a high count, which is the warning time. Energy also has obvious characteristics in the middle and late stages of this stage. The accumulation of high-energy signals is accompanied by sustained, steady, and rapid growth of energy. A large number of high-energy signals appeared at the moment of rock sample rupture. The biggest difference between sz-22 and sz-21 is the width of the sound emission band and the frequency of energy release. The sz-22 acoustic emission count shows a narrow band to the wide band, and the sz-21 acoustic emission count shows a wide band to the narrow strip development. The sz-22 acoustic emission energy is released in a concentrated manner, presenting a few high-energy events, and the sz-21 acoustic emission energy is continuously released, presenting multiple high-energy events. The rupture pattern of the rock sample in Figure 12 also shows that sz-22 forms a through-shear main crack and a local shear microcrack, and sz-21 forms a lower shear main crack and an upper pull crack, which is the combined shear-pull crack. The alternating occurrence of the composite crack leads to the continuity of the high-energy signal and the total amount of the count is gradually reduced, and the partial shear crack gradually expands to cause the discontinuity of the high-energy signal, and the total amount of the count gradually increases. Accordingly, the type of the final rupture crack can be determined by the

Table 2: Early warning table of body strain precursory information.

Numbering of rock samples	Peak stress (MPa)	Peak time (s)	Volume minimum strain (%)	Volume minimum strain time (s)	Precursory warning time (s)	Percentage of total time in advance (%)	Average value (%)
sz-17	103	1219	0.93	1080	139	11.4	
sz-18	113	1316	1.04	1177	139	10.6	
sz-20	105	1223	0.85	1085	138	11.3	11.4
sz-21	107	1270	0.85	1106	164	12.9	
sz-22	106	1245	0.78	1103	142	11.4	

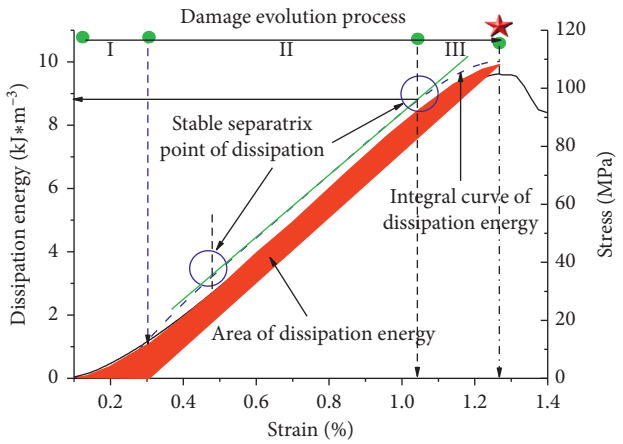

Figure 7: Relationship curves between strain stress and dissipative energy damage evolution process by sz-20.

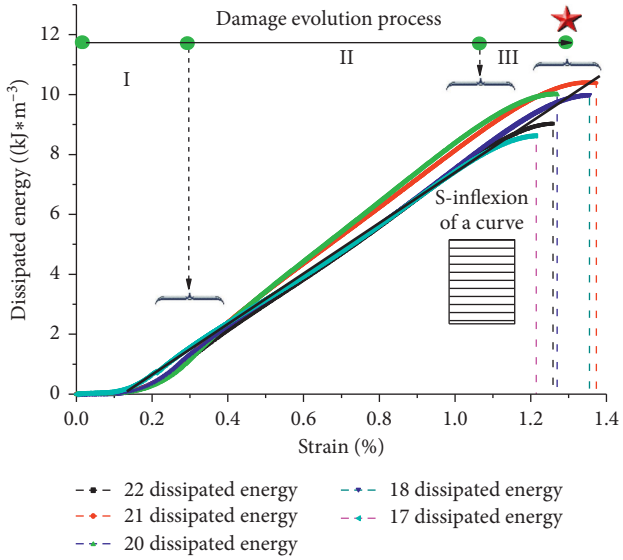

Figure 8: Relationship curves between strain and dissipative energy damage evolution process.

overall increase in the acoustic emission count and the continuity of the acoustic emission energy release.

The sz-22 and sz-21 curves are taken as examples to illustrate the acoustic emission count and energy precursor recognition effects. The sz-22 rock sample has a failure time of 1241 s, the corresponding pressure value is 106 MPa, and the sound emission high count boundary point is set to 1000 (yellow appearance area), the corresponding time is 1002 s, and the rupture occurs 243 s ahead of time for early warning. The warning time for loading to the destruction process is 19.5%. When the high-energy demarcation point of the acoustic emission is set to high-energy continuous occurrence and accelerated growth, the corresponding time is 1115 s, and the early warning is 130 s ahead of the damage for early warning, and the relative loading time to the destruction process is 10.5%. The sz-21 rock sample has a failure time of 1270 s, and the corresponding pressure value is 107 MPa. The time corresponding to the sound emission high-counting boundary point is 927 s, and the warning occurs 240 s ahead of the disaster, and the relative loading time to the damage process is 18.9%. The time corresponding to the high energy of acoustic emission is 1013 s, and the early warning is 154 s ahead of the damage, and the warning time is 12.1%. Other rock samples have similarities and will not be described here.

3.4. Acoustic Emission Average-Frequency and Peak-Frequency Damage Precursor Analysis. The acoustic emission signal is a wave signal. Fourier transform is an effective way to process the wave signal. Converting the signal from the time domain to the frequency domain and exploring the characteristics of the waveform from another angle help us to find the precursor information of the rock damage process. Taking the acoustic emission waveform near the peak of the sz-22 rock sample as an example, the original waveform is transformed into the frequency domain by fast Fourier transform. The original waveform is subjected to wavelet denoising processing. As shown in Figure 13(a), the origin-analysis-signal-FFT is input, and the amplitude and phase change with frequency are obtained, as shown in Figure 13(b).

In this paper, the Fourier transform is performed on all the acoustic emission waveforms collected, and the variation law of the peak-frequency rock sample damage evolution process is analyzed. According to Figure 9, the relationship between the average frequency and the count and duration is obtained. The average frequency variation law during loading to failure is determined by waveform analysis, and the rock damage precursor information is studied by the average frequency and the peak frequency.

Figure 14 shows the variation of the average frequency and peak frequency of the rock sample sz-22 during the loading process. It is found that the peak frequency is obviously partitioned, and its range and accumulation are divided into low-frequency zone, medium frequency zone, and high-frequency zone. The distribution of low-frequency

Table 3: Dissipative energy table of body strain precursory information.

Numbering of rock samples	Dissipation energy inflection point (kJ/m^3)	Corresponding moments (s)	Precursory warning time (s)	Percentage of total time in advance	Average value (%)
sz-17	7.82	1124	95	7.8	
sz-18	9.52	1215	101	7.7	
sz-20	9.57	1132	91	7.4	7.8
sz-21	9.93	1170	100	7.9	
sz-22	8.68	1144	142	8.1	

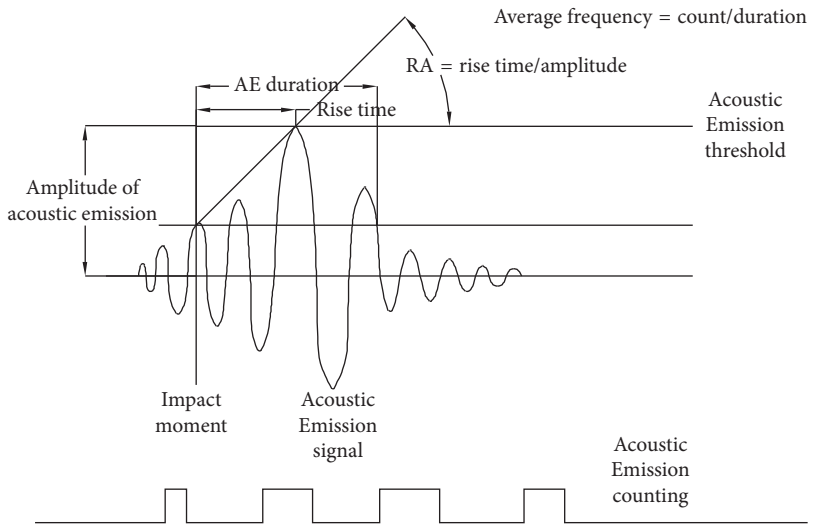

Figure 9: The principle of acoustic emission parameters calculation based on wave velocity.

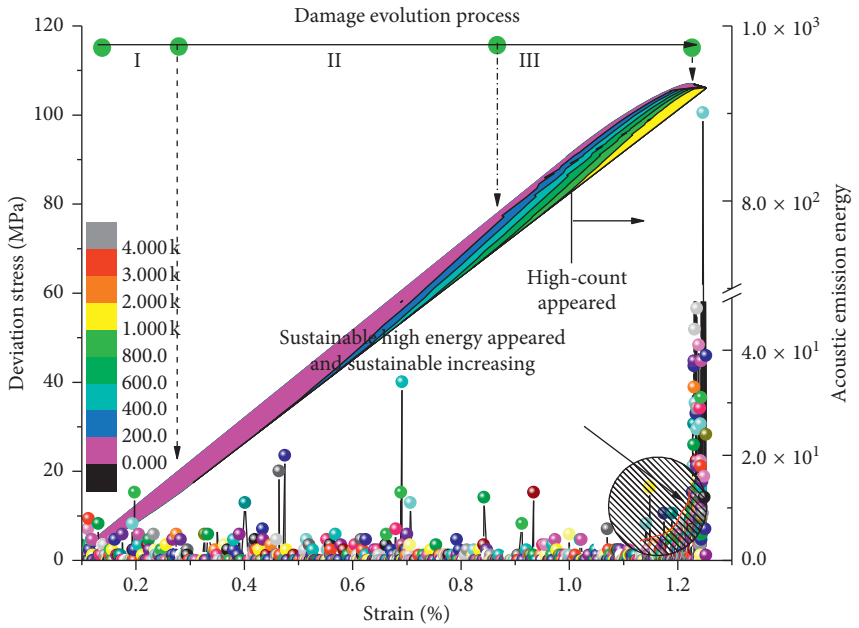

Figure 10: Partial stress-strain acoustic emission counting: acoustic emission energy damage evolution process by sz-22.

signals is in the whole process of damage evolution. There are few low-frequency signals in the early stage of damage evolution and intense stage of damage evolution, and the distribution of the middle stage of damage evolution is the intermediate frequency signal, which is accompanied by the whole process of damage evolution, and the whole is persistent and stable, and a large number of middle frequency signals only appear in the early stage of damage; high-frequency signals only appear in the middle and severe stages of damage evolution. The high-frequency signals in the early stage of damage evolution are sparse. The high-frequency signals in the middle and late stages of damage

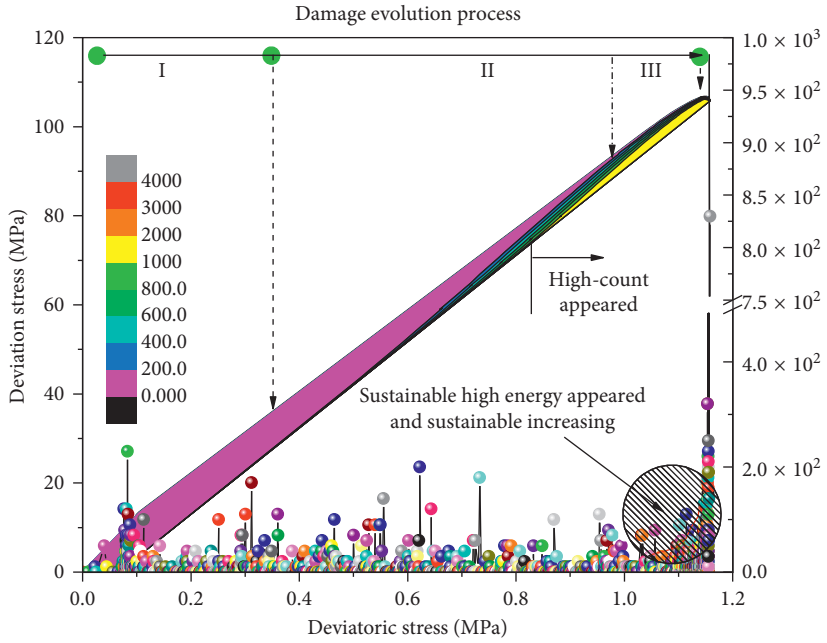

Figure 11: Partial stress-strain acoustic emission counting: acoustic emission energy damage evolution process by sz-21.

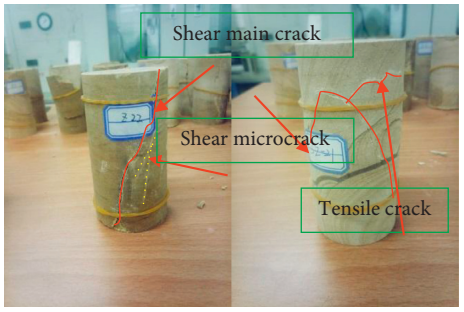

Figure 12: Fracture morphology by sz-22 and sz-21.

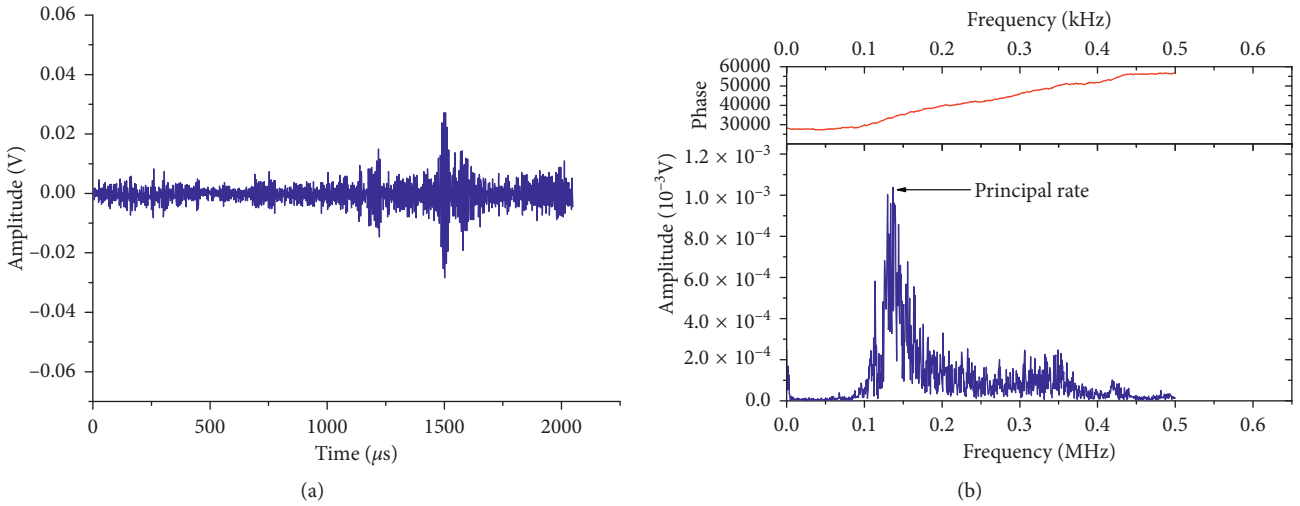

Figure 13: Fourier time-frequency transformation. (a) Waveform signal. (b) Two-dimensional spectrogram.

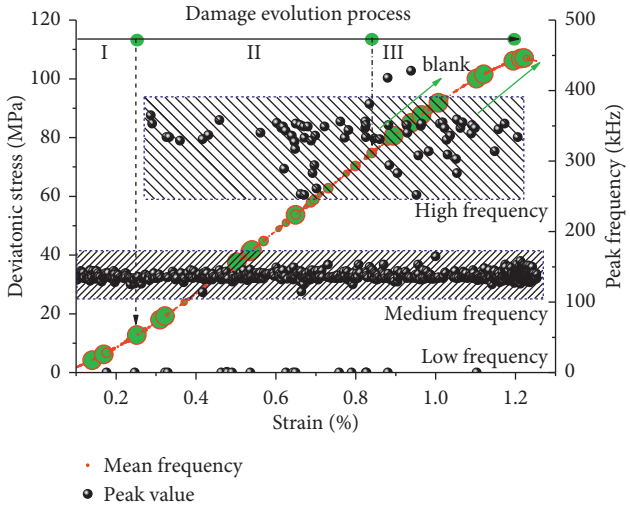

Figure 14: Damage evolution of peak frequency and average frequency by sz-22.

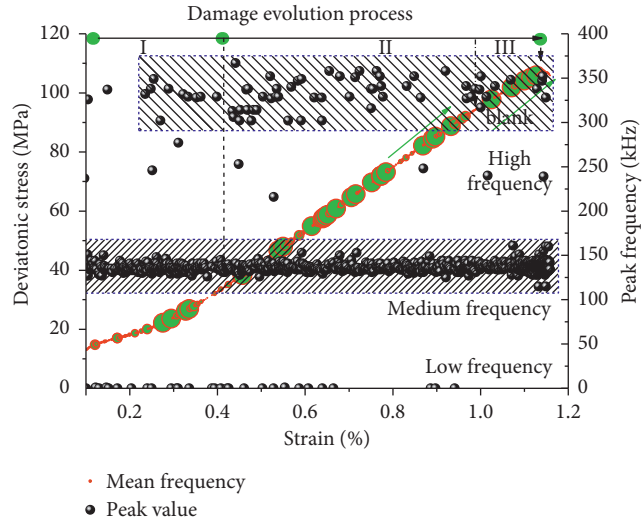

Figure 15: Damage evolution of peak frequency and average frequency by sz-21.

evolution are more stable and stable. The signal is more and stable, and the high-frequency signal shows a significant decreasing trend in the late stage of the violent evolution. It is concentrated in the middle. Through the above analysis, the rupture can be predicted by the increase of the high-frequency signal and the decrease of the high-frequency signal.

In Figure 14, the red and the green circle size represent the average frequency value. The curve trend is the stress-strain trend. As the degree of damage evolution increases, the average frequency exhibits high numerical accumulation at only a few points, which is consistent with the expansion of microcracks in the previous section. In the violent stage of damage evolution, there are obvious hierarchical features. In the first stage, a high-average frequency signal appeared, and it was stable and continuous. There was a clear blank period in the middle. At this time, the average frequency was extremely low, and then the high-average frequency signal continued to appear until the sample was destroyed. Therefore, the continuous appearance of the signal with a high-average frequency blank continues to appear as a precursor to destruction. Figure 15 is similar to the overall law of Figure 14. The average frequency of sz-22 presents an intermittent high value, and the average frequency of sz-21 shows a continuous high value, and the crack type analysis shows consistency.

In summary, sz-22 is taken as an example to illustrate the precursor characteristics of average-frequency and peak-frequency destruction. The average frequency warning has the law of continuous high value-no-sustained high value. In order to accurately find and judge the early warning point, the blank period or the end of the quiet period is used as the early warning point; that is, when the high-average frequency signal continues to appear again, the corresponding strain at this time and the time of the moment are 1.08% and 1058s, which is 102 s ahead of the disaster, and the warning time from the relative loading to the damage process is 8.2%. The peak frequency is sparse in the high-frequency signal in the early stage of the destruction. The medium- and high-frequency signals suddenly increase, which can judge the coming of the destruction. At this time, the strain and time are 1.16% and 1122 s, the damage is 45 s ahead of the damage, and the relative loading time to the damage process is 3.6%.

3.5. Acoustic Emission b Value and Sample Entropy Precursor Analysis. The waveform signal carries information about the interior and propagation path of the rock. Deep and reasonable excavation will better understand and grasp the state of the rock sample, and infer or evaluate the stability of the rock mass. The value of b can better characterize the scale of rock crack propagation. Scholars have found that the occurrence of large-scale rupture will lead to the decrease of b value, so as to study the crack propagation and extension and penetration process. Sample entropy can evaluate the degree of chaos in the chaotic state of the system and is a key indicator for system stability evaluation. The crack propagation of rock has disorder, the acoustic emission signal is consistent with crack propagation, and the change of entropy is related to the degree of disorder. The smaller the entropy is, the lower the degree of chaos is. The increase of entropy indicates the crack of rock sample. The increased disorder increases, and the crack is active, indicating that the distance damage is getting closer. The evolution process of rock damage is the evolution of a regular, orderly state toward an irregular and disordered state.

3.5.1. Analysis of b Value. By analyzing the variation law of b value, the precursor characteristics of coal rock damage are revealed. In this paper, the least square method is used to calculate the acoustic emission b value, and the magnitude is selected as 2 dB. To avoid the acoustic emission data, the error of the b value is calculated. The window length is 200, and the sliding distance is 100.

Figure 16 shows the variation of the b value during the loading of the sample 22 to the failure process. In the figure, the sphere is a three-dimensional coordinate system, which

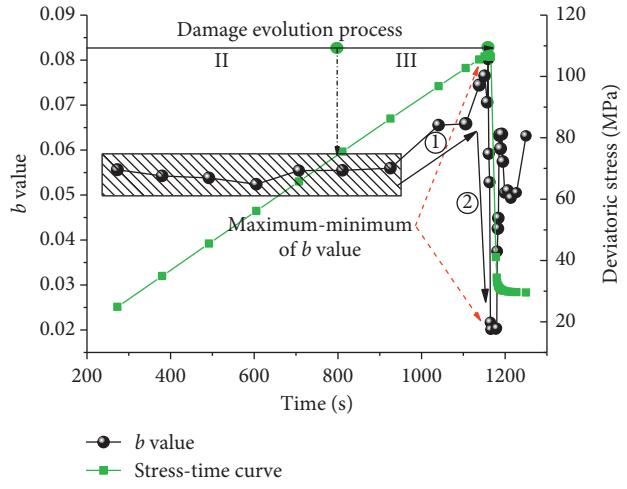

Figure 16: Stress time b value correlation change rule sz-22.

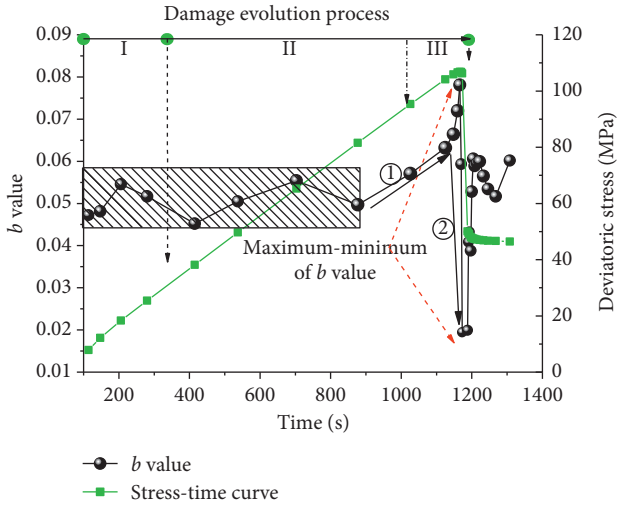

Figure 17: Stress time b value correlation change rule sz-21.

represents time, b value, and correlation. The diameter of the sphere is correlation. Since the correlation is between 0.8 and 0.9, the diameters of the sphere are not much different, which also indicates the correlation of the data is better. The b value is more obvious during the whole process of change. The initial b value of the damage evolution stage and the initial stage of the damage evolution fluctuate within the range of 0.05~0.06, indicating that the scale of crack propagation is stable at this time. This conclusion is similar to the variation of dissipative energy. From then on to the prerupture period, the b value showed a significant growth trend and reached the peak value and then instantaneously dropped to the minimum value. During the ascent, the b value is like stepwise, the middle showed a short-term platform, and then rapidly increased to the maximum value, and the maximum b value was 0.079. This stage is the process of microcrack accumulation and is the basis of crack penetration. The b value appears to decrease rapidly and continuously, indicating that the microcracks penetrate to form cracks, and the cracks penetrate to form the main control crack. What follows is the occurrence of rupture. The consistency of the whole process is better. It is risky to use the decrease of b value as the rupture of precursor information. It is proposed to use the rise of b value as the early warning point. The variation rule of Figure 17 is consistent with Figure 16 and only differs in specific parameters. The b value of the initial stage and the midterm of the damage evolution fluctuated between 0.045 and 0.06, which was larger than the fluctuation range and volatility of the sample 22. It indicates that the composite crack has a certain influence on the b-value change. The b-value rise period continues to be stable, and the whole process from stable to rapid indicates that the microcracks show a growing trend, and the b-value decreases rapidly at the time of rupture.

In summary, sz-22 and sz-21 are taken as examples to illustrate the precursor characteristics of crack rupture scale. The b-value warning has the law of steady-rapid growth-sudden drop. In order to accurately find and judge the early warning point, the growth starting point is the early warning point. The b-value and time corresponding to sz-22 are 0.056 and 929 s, and the damage is 231 s ahead of time. The warning time for loading to the destruction process is 18.6%. The b value and time corresponding to sz-21 are 0.049 and 878 s, the damage is 289 s ahead of the damage, and the relative loading time to the damage process is 22.8%.

3.5.2. Calculation Method and Analysis of Sample Entropy. The process of rock damage evolution is a simple-to-complex process. The sample entropy can measure the complexity of time series, especially for nonlinear dynamics. The sample entropy can obtain more accurate values without higher data length and consistency. The methods are as follows:

Suppose the original data is a time series from 1 to N, expressed as $\{u(i) : 1 \le i \le N\}$.

(1) First construct the m-dimensional vector group as follows:

$$X(1),\ X(2), \ldots, X(N-m+1), \tag{1}$$

where $X(i) = \{u(i),\ u(i+1), \ldots, u(i+m)\}$

(2) Find the distance between the vector group$X(i)$ and $X(j)$, where is the vector maximum difference group, i.e.,

$$d[X(i),\ X(j)] = \max_{k=0\sim m-1} |u(i+k) - u(j+k) \tag{2}$$

(3) When analyzing each $\{i : 1 \le i \le N-m+1\}$, assume that the deviation is r, the number of statistical vector groups is less than r, which is counted as $Nm(i)$. Analyzing the ratio of the quantity less than r to the total number is $C_i^m(r) = N_m(i)/(N-m)$, where the average value of i can be expressed as $\phi^m(r)$, which is $\phi^m(r) = (1/N-m)\sum_{i=1}^{N-m} C_i^m(r)$

As the dimension changes, repeat steps (1)–(3) above to get $C_i^{m+1}(r)$, $\phi^{m+1}(r)$:

$$C_i^{m+1}(r) = \frac{N_{m+1}(i)}{(N-m+1)},$$
$$\phi^{m+1}(r) = \frac{1}{N-(m+1)} \sum_{i=1}^{N-(m+1)} C_i^{m+1}(r). \quad (3)$$

Based on the above theory, the sample entropy expression relationship is related to N, m and r parameters, SampEn$(N,\ m,\ r)$:

$$\text{SampEn}(m,\ r) = \lim_{N \longrightarrow} \left\{-\ln\left[\frac{\phi^{m+1}(r)}{\phi^m(r)}\right]\right\}. \quad (4)$$

The amount of data cannot be infinite, and N takes a finite number based on the experimental results and estimates:

$$\text{SampEn}(N,\ m,\ r) = -\ln\left[\frac{\phi^{m+1}(r)}{\phi^m(r)}\right]. \quad (5)$$

The data amount N, the dimension m and the tolerance r are combined to obtain the sample entropy, so if the above parameters are different, the obtained sample entropy is also different. After long-term research by scholars, it is found that when r takes 0.1~0.25 times of the standard deviation of the original data, the value of $SampEn(N,\ m,\ r)$ has the best dependence on the length N of the sequence when $m = 1$, and the calculated sample entropy has reasonable statistical characteristic.

Based on the above mechanism, the MATLAB program was developed to analyze the entropy of the waveforms in the early, middle, and severe stages of the damage evolution. The time-based fitting found that with the increase of stress, the sample entropy is ordered, chaotic and disordered, and ordered. Specifically, the analysis is carried out with sz-22 and sz-20.

Figure 18 shows the variation of sample entropy during the damage evolution of rock sample 22. In the early and middle stages of damage evolution, the rock sample is always in an orderly state (entropy fluctuates in a small range), and the rock sample is in a stable state. Crack initiation is also less and regular. The upper limit of the orderly stage is reached in the early stage of the violent evolution of the damage, indicating that it is developing to the chaotic period. The sample entropy in the middle stage of the violent evolution has a strong fluctuation, and it changes between order and disorder, indicating that the crack has begun to extend, and its number begun to increase. In the early stage of rupture, the sample entropy suddenly increased and then suddenly decreased. The maximum value of the rise reached 5.23, and the minimum value reached 2.53, indicating that the internal crack of the rock sample was adjusted to the ordered state immediately after the chaos, and the cracks were disorderly arranged to the ordered self-organized arrangement, indicating the formation of the master crack. After the peak, the sample entropy is adjusted to an ordered state. To sum up the above process, the beginning of chaos and the beginning of disorder should be used as the demarcation point of the prejudgment. By analyzing the sz-21 sample entropy along with the damage evolution process, the two have similarities and are not specifically analyzed.

In summary, sz-22 and sz-20 are taken as examples to illustrate the precursor characteristics of sample entropy.

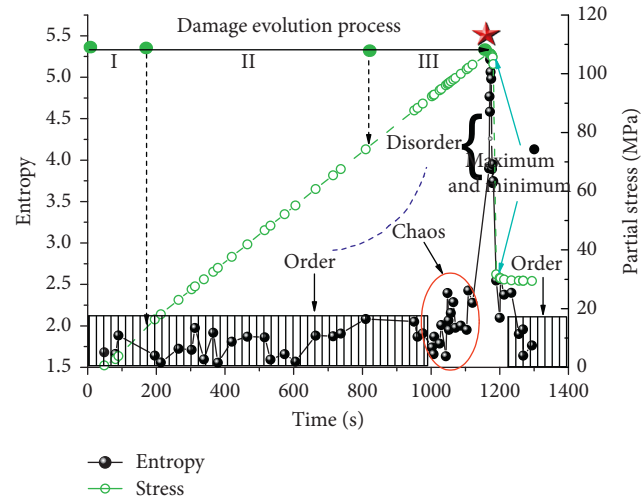

Figure 18: The variation law of sz-22 stress time entropy value.

The rock sample 22 entropy of Figure 19 early warning has order-chaos-disorder-ordered law. In order to accurately find and judge the early warning point, the sample entropy early warning has order-chaos-disorder-ordered law. In order to accurately find and judge the early warning point, the chaotic end point and the disordered starting point are used as the early warning points. The corresponding sample entropy value and time of sz-22 at this time are 2.4 and 1124 s. It was 41 s ahead of the damage, and the relative loading time to the damage process was 3.3%. At this time, the corresponding sample entropy and time of sz-20 are 2.5 and 1119 s. It is 36 s ahead of the damage, and the relative loading time to the damage process is 2.9%.

Through the analysis of the above index selection process, each index has representativeness and certain meaning, but the selection of a single index as a rupture forecast is one-sided and misunderstood. In the process of rock damage evolution, the information fed back in different stages is not consistent. Multiple indicators should be selected for simultaneous forecasting. The precursor information of each stage or the precursor information of different angles in the same stage should be grasped. From the perspective of time order, the rock instability of destruction can be accurately predicted by comprehensive evaluation. This paper analyzes eight indicators from four angles, which is comprehensive. The body strain and dissipated energy are selected from the perspective of rock mechanics. The counting and energy are selected from the acoustic emission timing parameters, and from the acoustic emission frequency domain. The average frequency and peak frequency are selected. The b value and sample entropy are selected from the acoustic emission characteristic parameters. The purpose and significance of the selection of each parameter is discussed. Take sz-22 as an example to illustrate the precursor characteristics of each parameter in the process of damage evolution.

By analyzing the body strain, dissipated energy, acoustic emission count, acoustic emission energy, average frequency and peak frequency and b value, and sample entropy prediction time percentage of Figure 20, it can be found that

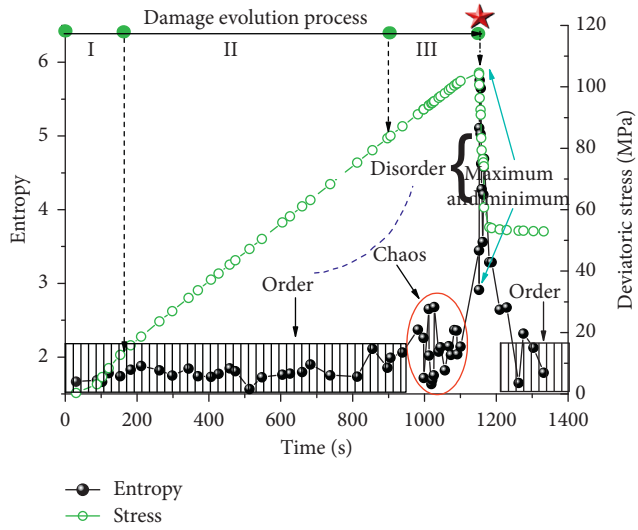

Figure 19: The variation law of sz-20 stress time entropy value.

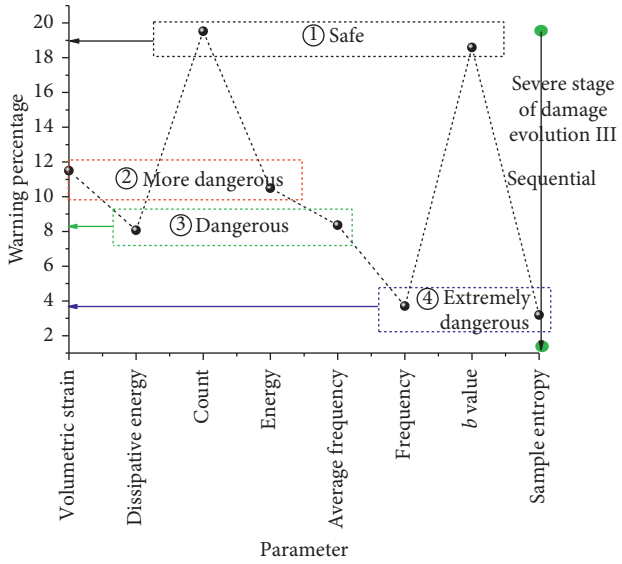

Figure 20: Parameter timing characteristics by sz-22.

there is a recessive correlation between parameters. The forecast time is divided into groups, and the similar time is divided into a group, which is divided into 4 groups. The first stage of feedback is the acoustic emission count and b value, the warning time is about 19%; the second stage is the feedback of the body strain and acoustic emission energy, the warning time is about 11%; the third stage makes feedback for the dissipated energy and average frequency, the warning time is about 8%; the fourth stage is the peak frequency and sample entropy, and the warning time is about 3%. By segmenting the damage evolution process, it is found that the early warning indicators have entered the stage of severe damage evolution (III), indicating the rightness of the selection of indicators. Table 4 gives the warning percentages of other groups of data acoustic emission count, b value, body strain, acoustic emission energy, dissipated energy, average frequency, peak frequency, and sample entropy. Each parameter satisfies the law proposed in Figure 20, indicating the accuracy of the method. The parameters of the gradient at the same time can be mutually verified, and the indicators of different gradients can characterize the degree of warning. According to the position of the indicator, it is divided into five levels: $1 \geq x$ is safe; $1 < x \leq 2$ is more dangerous; $2 < x \leq 3$ is dangerous; $3 < x \leq 4$ is urgent danger; $4 < x$ is emergency alarm.

4. Conclusion

The triaxial acoustic emission experiment of yellow sandstone was carried out by using TOP INDUSTRIE rock triaxial rheometer and SH-II acoustic emission system. Based on the rock damage evolution process, from the rock mechanics, acoustic emission time domain, frequency domain, and characteristic parameters, the rock damage precursors were analyzed, and a time series-based index fusion system was established.

(1) For the body strain, it is nearly linear in the local damage evolution stage (I and II); in the severe damage evolution stage (III), the body strain slope is from positive to negative, and the negative slope shows that a certain acceleration growth trend until the maximum is reached, and then the rock sample was destroyed. Considering the selectivity and desirability of the precursor information, the slope's zero-point end point is defined as the precursor information identification point.

(2) The dissipative energy curve shows the "s" type as a whole, and the growth rate in the early stage is fast-intermediately stable—the later period is slowed down. The boundary point of the upper slope of the "s" type curve is used as the precursor information.

(3) In the early stage of damage evolution,the AE count is small, and the local centralized jump occurs; in the middle of damage evolution, the proportion of high-counting signals gradually increases, and the

Table 4: Comprehensive index warning table.

Numbering of rock samples	Acoustic emission counting (N)	b value	Body strain (%)	Acoustic emission energy	Dissipative energy (kJm^{*-3})	Average frequency (kHz)	Peak frequency (kHz)	Sample entropy
sz-17	19.3	20.1	11.4	10.1	7.8	8.6	3.4	2.5
sz-18	18.7	19.6	10.6	9.8	7.7	9.1	3.1	2.7
sz-20	19.4	21.3	11.3	11.4	7.4	8.4	3.8	2.9
sz-21	18.9	22.8	12.9	12.1	7.9	8.1	3.2	3.0

number of low-counting signals becomes less and less in the stage of severe damage evolution. The layered features of the acoustic emission count are more and more obvious, and the specific gravity shift is more obvious. A high count appears as a precursor information identification point.

(4) In the violent stage of damage evolution, high-energy signals appear in the energy accumulation and accompany the continuous and steady growth of energy, which serves as a precursor information identification point.

(5) The effects of shearing main crack, shear micro-crack, tensile crack, and composite crack on the acoustic emission count and energy in the damage evolution stage are analyzed.

(6) Mid-low-frequency signal distribution: In the whole process of damage evolution, a large number of medium- and high-frequency signals appear in the early stage of damage; in the late stage of severe damage evolution, the high-frequency signal shows a significant decreasing trend and is concentrated in the middle. It is possible to predict the onset of rupture by an increase in the medium- and high-frequency signals and a decrease in the high-frequency signal.

(7) In the severe stage of damage evolution is the continuous occurrence of high-rate-blank-continuous high-frequency, and the end point of blank period as the precursor of destruction.

(8) The b value of acoustic emission fluctuates within a small range in the early and middle stages of damage evolution, and the period of severe damage evolution continues to increase steadily to rapid growth, with the starting point of sustained and stable growth as the damage identification point.

(9) In the process of damage evolution, the sample entropy presents an orderly, chaotic, disordered, and orderly process. The end of chaos and the beginning of disorder are used as the demarcation point of the prejudgment.

(10) Based on the time series, an eight-parameter comprehensive early warning system is constructed. The early warning indicators are in the stage of severe damage evolution and are classified into five levels for early warning.

Data Availability

The data used to support the findings of this study are available from the corresponding author upon request.

Conflicts of Interest

The authors declare that they have no conflicts of interest.

Acknowledgments

This research was supported by the National Natural Science Foundation of China (51574115, 51774121, 51674107, and 51604100). The authors would like to thank all members for their help with the fieldwork in Heilongjiang Ground Pressure & Gas Control in Deep Mining Key Lab (GPGC).

References

[1] Z. Cao, Y. Yang, Y. Wan et al., "Study on the precursors characteristics of acoustic emission and RFPA simlation in the process of brittle fracture of granite," *Mining R&D*, vol. 38, no. 2, pp. 25–29, 2018.

[2] X. Yao, Y. Zhang, X. Liu et al., "Optimization method for key characteristic signal of acoustic emission in rock fracture," *Rock and Soil Mechanics*, vol. 39, no. 1, pp. 375–384, 2018.

[3] H. Xu, *Acoustic Emission Characteristics and RFPA Simulation of Brittle Fracture of Rock*, Jiangxi University of Science and Technology, Jiangxi Sheng, China, 2017.

[4] Z. Shen, *Study On Infrared Acoustice mission Characteristics Of Coal Mass Failure Precursor Under Water Injection Condition*, Heilongjiang Institute of Science and Technology, Harbin, China, 2016.

[5] G. Liu, F. Xiao, G. Hu et al., "Analysis of rock burst hazard of righ three high level drainage roadway in lishu coal mine with ARES-5/E Ground sonic system," *Coal Mining Technology*, vol. 22, no. 03, pp. 65–69, 2017.

[6] G. Liu, Y. Zhang, Z. Shen et al., "Granite damage acoustic emission evaluation," *Journal of Heilongjiang University of Science and Technology*, vol. 25, no. 6, pp. 615–620, 2015.

[7] Y. Zhang, G. Yu, B. Tian et al., "Identification of multiple precursor information of acoustic emission dominant frequency in the process of granite failure," *Journal of Mining and Safety Engineering*, vol. 34, no. 2, pp. 355–362, 2017.

[8] Y. Zhang, P. Liang, B. Tian et al., "Multi parameter coupling analysis of acoustic emission signals of granite disaster and the precursor characteristics of the main rupture," *Chinese Journal of Rock Mechanics and Engineering*, vol. 35, no. 11, pp. 2248–2258, 2016.

[9] Y. Zhang, X. Liu, Z. Liang et al., "Experimental study of rockburst precursor of granite tunnel based on multi-physical

field parameters," *Chinese Journal of Rock Mechanics and Engineering*, vol. 33, no. 7, pp. 1347–1357, 2014.

[10] P. Zeng, Y. J. Liu, H. G. Ji et al., "Coupling criteria and precursor identification characteristics of multi-band acoustic emission of gritstone fracture under uniaxial compression," *Chinese Journal of Geotechnical Engineering*, vol. 39, no. 3, pp. 509–517, 2017.

[11] X. X. Liu, Y. B. Zhang, Z. Z. Liang et al., "Recognition of frequency information in acoustic emission monitoring of rock fracture," *Chinese Journal of Geotechnical Engineering*, vol. 39, no. 6, pp. 1096–1105, 2017.

[12] Y. Cong, X. T. Feng, Y. R. Zheng et al., "Experimental study on acoustic emission failure precursors of marble underdifferent stress paths," *Chinese Journal of Geotechnical Engineering*, vol. 38, no. 7, pp. 1193–1201, 2016.

[13] P. Zhang, *Study on Precursory Law prior to Rock failure based on Acoustic Emission Time Order*, Northeastern University, Boston, MA, USA, 2015.

[14] H. Ji, and X. Lu, "Characteristics of acoustic emission and rock fracture precursors of granite under conventional triaxial compression," *Chinese Journal of Rock Mechanics and Engineering*, vol. 34, no. 4, pp. 694–702, 2015.

[15] S.-Q. Yang, H.-W. Jing, and S.-Y. Wang, "Experimental investigation on the strength, deformability, failure behavior and acoustic emission locations of red sandstone under triaxial compression," *Rock Mechanics and Rock Engineering*, vol. 45, no. 4, pp. 583–606, 2012.

[16] Y. Zhang, Z. Yang, X.-L. Yao et al., "Experimental study of rockburst early warning method based on acoustic emission cluster analysis and neural network identification," *Rock and Soil Mechanics*, vol. 38, no. S2, pp. 89–98, 2017.

[17] Y. Zhang, peng Liang, X. Liu et al., "Experimental study on precursor of rock burst based on Acoustic emission signal dominant-frequency and entropy," *Chinese Journal of Rock Mechanics and Engineering*, vol. 34, no. S1, pp. 2959–2967, 2015.

[18] Q. Liu, R. Zhang, M. Gao et al., "Acoustic emission characteristics and comprehensive failure precursors of coal under unloading conditions," *Journal of Sichuan University (Engineering Science Edition)*, vol. 48, no. S2, pp. 67–74, 2016.

[19] J. Wei, S. Liu, L. Wu et al., "Comparative analysis on different AE parameters in biaxial loading of hole rock," *Journal of Mining and Safety Engineering*, vol. 32, no. 6, pp. 1017–1025, 2015.

[20] J. Wei, *Experimental Study on Joint Monitoring with Infrared and AE Technology in Rock Failure Process*, Northeastern University, Boston, MA, USA, 2014.

[21] LV. Yukai, *Study of Precursory Rules with Multi-Parameters Monitoring for Coal Mass Instability Destruction*, China University Of Mining And Technology, Xuzhou, China, 2012.

[22] Y. Zhao, L. Liu, Y. Pan et al., "Experiment study on microseismic, charge induction,self-potential and acoustic emission during fracture process of rocks," *Chinese Journal of Rock Mechanics and Engineering*, vol. 36, no. 1, pp. 107–123, 2017.

[23] Lei, "Seismic *b*-value for foreshock AE events preceding repeated stick-slips of pre-cut faults in granite," *Applied Sciences*, vol. 8, no. 12, p. 2361, 2018.

[24] M. Hu, H. Zhou, Y. Zhang et al., "Acoustic emission monitoring on damage evolution of surrounding rock during headrace tunnel excavation by TBM," *European Journal of Environmental and Civil Engineering*, no. 1, pp. 1–17, 2017.

[25] F. Xiao, G. Liu, T. Qin et al., "Acoustic emission (AE) characteristics of fine sandstone and coarse sandstone fracture process under tension-compression-shear stress," *Chinese Journal of Rock Mechanics and Engineering*, no. S2, pp. 3458–3472, 2016.

[26] F. Xiao, G. Liu, Z. Sehn et al., "Energy conversion and acoustic emission (AE)characteristics of coal samples under cyclic loading," *Chinese Journal of Rock Mechanics and Engineering*, vol. 35, no. 10, pp. 31954–1964, 2016.

[27] F. Xiao, G. Liu, Z. Shen et al., "Research on effective elastic energy release rate of taoshan #90 coal seam," *Chinese Journal of Rock Mechanics and Engineering*, vol. 34, no. S2, pp. 4216–4225, 2015.

[28] F. Xiao, Z. Shen, G. Liu et al., "Relationship between hysteresis loop and elastoplasticstrain energy during cyclic loading and unloading," *Chinese Journal of Rock Mechanics and Engineering*, vol. 33, no. 9, pp. 1791–1797, 2014.

[29] S. Q. Yang, "Experimental investigation on mechanical damage characteristics of sandstone under triaxial cyclic loading," *Geophysical Journal International*, vol. 201, no. 2, pp. 662–682, 2015.